

Soft Matter

Accepted Manuscript



This is an *Accepted Manuscript*, which has been through the Royal Society of Chemistry peer review process and has been accepted for publication.

Accepted Manuscripts are published online shortly after acceptance, before technical editing, formatting and proof reading. Using this free service, authors can make their results available to the community, in citable form, before we publish the edited article. We will replace this *Accepted Manuscript* with the edited and formatted *Advance Article* as soon as it is available.

You can find more information about *Accepted Manuscripts* in the [Information for Authors](#).

Please note that technical editing may introduce minor changes to the text and/or graphics, which may alter content. The journal's standard [Terms & Conditions](#) and the [Ethical guidelines](#) still apply. In no event shall the Royal Society of Chemistry be held responsible for any errors or omissions in this *Accepted Manuscript* or any consequences arising from the use of any information it contains.

Cite this: DOI: 10.1039/c0xx00000x

www.rsc.org/xxxxxx

ARTICLE TYPE

Structure-delivery relationships of lysine-based gemini surfactants and their lipoplexes

Mark Damen,^a Edgar Cristóbal-Lecina,^a Glòria Colom Sanmartí,^a Stijn F. M. van Dongen,^a Cristina L. García Rodríguez,^a Igor P. Dolbnya,^{b,#} Roeland J. M. Nolte,^a and Martin C. Feiters^{*a}

Received (in XXX, XXX) Xth XXXXXXXXXX 20XX, Accepted Xth XXXXXXXXXX 20XX

DOI: 10.1039/b000000x

The synthesis and properties of gemini surfactants of the type $(R^1(CO)-Lys(H)-NH)_2(CH_2)_n$ are reported. For a spacer length of $n = 6$, the hydrophobic acyl tail was varied in length ($R^1 = C8, C10, C12, C14, C16$, and $C18$) and, for $R^1 = C18$, the degree of unsaturation. For $R^1(CO) = \text{oleoyl}$ ($C18:1 Z$) the spacer length ($n = 2 - 8$) and the stereochemistry of the lysine building block were varied; a ‘half-gemini’ derivative with a single oleoyl tail and head group was also prepared. The potential of the gemini surfactants to transfer polynucleotides across a cell membrane was investigated by transfection of HeLa cells with beta-galactosidase, both in the presence and absence of the helper lipid DOPE. Oleoyl was found to be by far the best hydrophobic tail for this biological activity, whereas the effect of the lysine stereochemistry was less pronounced. The effect of an optimum spacer length ($n = 6$) was observed only in the absence of helper lipid. The most active surfactant, i.e. the one with oleoyl chains and $n = 6$, formed liposomes with sizes in the range of 60 – 350 nm, and its lipoplex underwent a transition from a lamellar to a hexagonal morphology upon lowering the pH from 7 to 3.

Keywords: gemini surfactant; gene delivery; electron microscopy; small-angle X-ray scattering

1. Introduction

Gemini surfactants are symmetrical surfactants featuring two sets of hydrophilic head groups and hydrophobic tails that are joined by a spacer [1]. Both flexible spacers and rigid spacers have been reported [2,3], and gemini surfactants generally have superior surfactant properties compared to their single head single tail analogues. For instance, increased surface activities of several orders of magnitude have been reported [4]. They also typically have critical micellar concentrations (CMCs) in the micromolar range, much lower than those of classical surfactants. These superior attributes make gemini surfactants promising candidates in studies of biomedical applications, because concentrations can be lowered to minimize toxicity without losing activity.

We have demonstrated previously [5] that cationic gemini surfactants, e.g. those based on tartaric acid [6], can be applied in transfection, i.e. the process of delivering a gene to a cell. The presence of multiple cationic groups in a single surfactant molecule and, at the same time, of multiple cationic surfactant molecules in a lipid aggregate both contribute to a strong binding of DNA due to a multivalency effect [7]. The mutual influence of the multiple protonable groups in a molecule and within an aggregate on each other's pK_a values leads to a pH-dependence of the DNA binding process, which stimulates endosomal escape when the lipid-DNA complex (or *lipoplex*) is taken up by a cell [8].

A promising class of gemini surfactants has the general description $(R^1(CO)-Lys(R^2)-NH)_2(CH_2)_n$ (shorthand notation $R^1\text{-Lys-}R^2\text{-}n$) and contains two moieties of the natural amino acid lysine (Lys represents the natural L-isomer unless explicitly indicated otherwise). These amino acids are acylated on their Σ -amino groups, and are coupled by a diamine linker between their carboxylic acid groups (Figure 1). Of the series (Oleoyl-Lys(H)-NH) $_2$ (CH $_2$) $_n$ (abbreviated as **OI-Lys-H-n**) with $n = 2, 4, 6$, or 8 , the compound with $n = 6$ (**OI-Lys-H-6**) was among the most active compounds in the transfection of Chinese hamster ovary (CHO) cells with luciferase, using LipofectAmine Plus[®] as a positive control [5]. The Arg analogues were the first representatives of this class of compounds [9], featuring antimicrobial activity, later also found for **C12-Lys-H6** [10,11].

We have recently [12] reported on transfection studies with the so-called geminoid **OI-SPKR-OI**, a compound related to gemini surfactants but more asymmetric, which is remarkably effective without the non-cationic lysogenic helper lipid dioleoylphosphatidyl ethanolamine (DOPE) usually required for transfection by lipids [13-15]. Interestingly, the preliminary results [5] indicated that transfection by **OI-Lys-H-n** also proceeds without helper lipid. We report here on the synthesis and some transfection, with and without helper lipid, and physicochemical properties of various compounds $(R^1(CO)-Lys(R^2)-NH)_2(CH_2)_n$, in which the acyl tail $R^1(CO)$, the stereochemistry of Lys, and the spacer length n were varied.

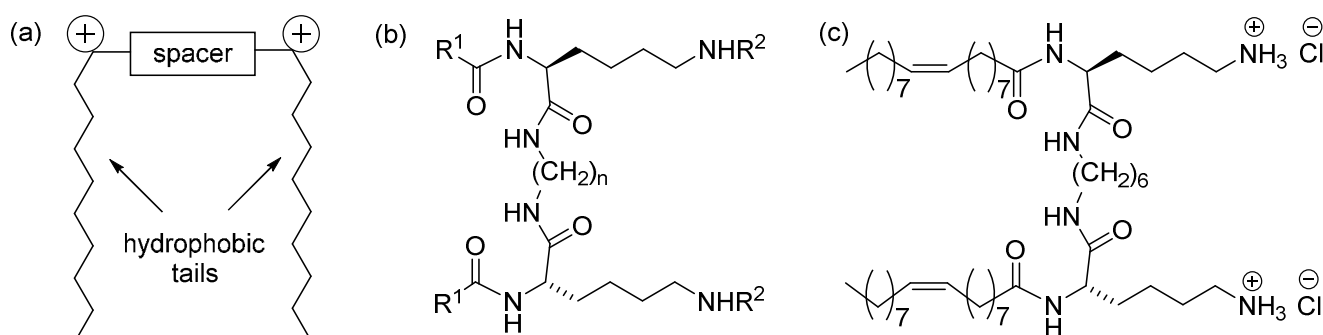


Figure 1. (a) Schematic representation of a cationic gemini surfactant. (b) General structure of $(R^1(\text{CO})\text{-Lys}(R^2)\text{-NH})_2(\text{CH}_2)_n$ (or $R^1\text{-Lys-}R^2\text{-}n$). (c) Full structure of the biologically active $(\text{Oleoyl-Lys}(\text{H})\text{-NH})_2(\text{CH}_2)_6$ or OI-Lys-H-6 .

2. Materials and Methods

2.1. General Procedures

THF was purified by distillation under nitrogen from sodium/benzophenone, dry acetonitrile was obtained by distillation under nitrogen from phosphorus pentoxide. Dry DMF was purchased from Fluka and anhydrous pyridine from Aldrich. Other chemicals were purchased from Aldrich, Fluka or Acros and used as received. Analytical thin layer chromatography (TLC) was performed on Merck precoated silica gel 60 F-254 plates (layer thickness 0.25 mm) and the compounds visualized by ultraviolet (UV) irradiation at $\lambda = 254$ nm and/or $\lambda = 366$ nm and by staining with phosphomolybdic acid reagent or KMnO_4 .

2.1.1. Nuclear magnetic resonance (NMR)

^1H NMR spectra were recorded at 25 °C on Varian Inova 400 or a Bruker DMX-300 machines operating at 400 and 300 MHz, respectively. ^{13}C NMR spectra were recorded on a Bruker DMX-300 machine operating at 75 MHz. ^1H NMR chemical shifts (δ) are reported in parts per million (ppm) relative to a residual proton peak of the solvent, $\delta = 4.79$ for D_2O , $\delta = 3.31$ for CD_3OD , $\delta = 7.26$ for CDCl_3 , and $\delta = 2.50$ for $\text{DMSO-}d_6$. Multiplicities are reported as: s (singlet), d (doublet), t (triplet), q (quartet), dd (doublet of doublets), ddd (doublet of doublet of doublets) or m (multiplet). Broad peaks are indicated by b. Coupling constants are reported as a J value in Hertz (Hz). The number of protons (n) for a given resonance is indicated as nH, and is based on spectral integration values. ^{13}C NMR chemical shifts (δ) are reported in ppm relative to a carbon peak of the solvent, $\delta = 49.0$ for CD_3OD , $\delta = 77$ for CDCl_3 and $\delta = 40$ for $\text{DMSO-}d_6$; when the solvent was D_2O , sodium-3-trimethylsilylpropionate-2,2,3,3- d_4 was added as internal standard, $\delta = 0.38$. The signals of the protons on hydroxyl, amino and carboxylic groups could not be observed due to the fast exchange with acids present in traces in the deuterated solvents. The resolution of ^{13}C spectra was increased when necessary by performing an exponential apodization of the FID.

2.1.2. Mass spectrometry (MS)

All the mass analyses were performed by using electrospray techniques (ESI). High-Resolution mass spectrometry measurements were performed on a JEOL AccuTOF instrument by using water, acetonitrile or methanol as solvents. Standard mass spectrometry measurements were performed on a

FINNIGAN LCQ Advantage Max by using water, acetonitrile or methanol as solvents.

2.1.3. High-performance liquid chromatography (HPLC)

High-performance liquid chromatography (HPLC) was carried out on a Shimadzu LC-20AT HPLC system equipped with a UV-Vis detector SPD-10AV and a fraction collector. Columns were purchased from Dr. Maisch GmbH. The compounds were purified on a mg scale by using a semipreparative reversed-phase column. A 2 mL solution was injected in a column ReproSil 100 C8, 5 μ (250 x 10 mm) operating at 30 °C. The detection wavelengths were fixed at 254 and 215 nm. A gradient of water and acetonitrile both containing either 0.1% v/v HCl or TFA was used as mobile phase, with a flow rate of 4 mL min^{-1} . HCl was used to ensure that the chloride was the only counterion of the isolated compounds. In all cases the samples were prepared by dissolving the compound in a suitable mixture water/acetonitrile and filtered on a nylon syringe filter (0.2 μm).

2.2. Synthesis

Details of the preparation of the target compound with $n = 6$ are given here; the experimental details of the preparations of its enantiomer, as well as of a classical (non-gemini) analogue, the compounds with $n = 2, 3, 4, 5$, and 8, with acyl tails varying in length (C8, C10, C12, C14, C16, and C18) and unsaturation (C18:1(Z), C18:1(E), C18:2(Z)), which were carried out analogously to that of the compound with $n = 6$, are given in the Electronic Supplementary Information.

2.2.1. Synthesis of (Z-Lys(Boc)-NH) $_2$ (CH $_2$) $_6$

Z-Lys(Boc)-OH.DCHA (dicyclohexylammonium) salt (3.0016 g, 5.343 mmol) was suspended in ethyl acetate (50 mL) and a few mL of a 10% KHSO_4 solution were added. The mixture was stirred for 15 minutes until all starting material had dissolved. Subsequently, extractions were carried out with H_2O and brine until a neutral pH was reached. The organic layer was dried with Na_2SO_4 and filtered. The solvent was removed and the remaining oil was dried *in vacuo*, yielding the free amino acid as a white foamy substance (1.9159 g, 93.9 %). This material was then dissolved in ethyl acetate saturated with water, and HOBT. H_2O (941.2 mg, 6.146 mmol), 1,6-diaminohexane (270.0 mg, 2.324 mmol), and EDC.HCl (1.154 g, 6.020 mmol) were added. A white precipitate was formed overnight. The suspension was extracted two times with a 10% aqueous Na_2CO_3 solution, once with H_2O , two times with an aqueous 10% KHSO_4 solution, once

with H₂O, two times with an aqueous 10% Na₂CO₃ solution, and once with brine, respectively. The precipitate was isolated by filtration and dried *in vacuo* in a desiccator. The organic layer of the extraction was evaporated and checked with TLC using CHCl₃:MeOH = 5:1 (v/v) as an eluent; this fraction was discarded as traces of both Z-Lys(Boc)-OH (Ninhydrin positive, R_f = 0.34) and HOBt (UV positive, R_f = 0.18) could be detected. (**Z-Lys(Boc)-NH₂(CH₂)₆**) was obtained as a white solid. Yield: 1.864 g (MW = 841.04, 95.4%), R_f = 0.63 (CHCl₃:MeOH=5:1). ¹H NMR (300 MHz, CDCl₃) δ: 7.33 (s, 10H, Z Ar), 6.51 (br s, 2H, diamine NH), 5.83 (br s, 2H, lysine α-NH), 5.04 (q, 4H, Z CH₂), 4.69 (br s, 2H, lysine ε-NH), 4.15 (m, lysine α-CH*), 3.29 (m, 2H, diamine 1,6-CH₂), 3.21 (m, 2H, diamine 1,6-CH₂), 3.07 (m, 4H, lysine ε-CH₂), 1.79 (m, 2H, lysine β-CH₂), 1.64 (s, 2H, lysine β-CH₂); 1.53 (br s, 4H, lysine δ-CH₂), 1.45 (s, 18H, Boc CH₃), 1.29-1.35 (m, 8H, diamine 2,3,4,5-CH₂); (m, 4H, lysine γ-CH₂). ¹³C NMR (300 MHz, CDCl₃) δ: 172.2, 156.2, 136.2, 128.5, 128.0, 79.1, 66.9, 55.0, 39.9, 38.2, 32.1, 29.5, 28.4, 24.9, 22.6. LCQ (ESI) calculated (C₄₄H₆₈N₆O₁₀): 840.5, found: 841.6 (M+H)⁺, 863.5 (M+Na)⁺, 1703.9 (2M+Na)⁺.

2.2.2. Synthesis of (Oleoyl-Lys(Boc)-NH)₂(CH₂)₆

(**Z-Lys(Boc)-NH₂(CH₂)₆**) (0.5014 g, 0.5962 mmol) was dissolved in 50 mL of DMF. The solution was filtered, collected in a round-bottomed flask and the palladium carbon catalyst (0.1 g) was added. After removal of all air from the round bottom flask, a hydrogen atmosphere was established using a balloon. The reaction was followed on TLC using BAW as an eluent and a ninhydrin solution as a staining agent. The starting material, the intermediate product with one Z protecting group left, and the final product could be distinguished very clearly with R_f values of 0.94, 0.74 and 0.46, respectively. When the hydrogenation was complete (typically after 1 or 2 hours) the DMF solution was filtered under suction over a P3 glass filter that was protected by Kieselguhr. To the DMF solution oleic acid (0.46 mL, 1.45 mmol), HOBt.H₂O (0.736 g, 4.81 mmol), and EDC·HCl (0.690 g, 3.61 mmol) were added. The mixture was left stirring overnight and the progress of the reaction was monitored by TLC using BAW as an eluent and a ninhydrin solution for staining. The product and a sideproduct with only one oleoyl tail appeared at R_f values of 0.94 and 0.67, respectively. When only product remained the DMF was evaporated and dried under high vacuum. The residue was dissolved in chloroform and extracted two times with a 10% aqueous Na₂CO₃ solution, two times with an aqueous 10% KHSO₄ solution, two times with an aqueous 10% Na₂CO₃ solution, and once with brine, respectively. After drying the organic layer over anhydrous sodium sulphate, filtering, solvent evaporation, and drying at an oil pump, the product was purified by column chromatography (eluent: 10 % methanol in chloroform), followed again by solvent evaporation and drying at an oil pump. (**Oleoyl-Lys(Boc)-NH₂(CH₂)₆**) was obtained as a white solid. Yield: 0.3095 g (MW = 1101.67, 47.12 %) R_f = 0.61 (CHCl₃:MeOH = 9:1). ¹H NMR (300 MHz, CDCl₃) δ: 6.93 (br t, 2H, diamine: NH), 6.77 (br d, 2H, lysine: α-NH), 5.34 (m, 4H, oleoyl: CH=CH), 4.79 (t, 2H, lysine: ε-NH), 4.47 (q, 2H, lysine: α-CH*), 3.35 (m, 2H, diamine: 1,6-CH₂), 3.10 (m, 2H, diamine: 1,6-CH₂); (m, 4H, lysine: ε-CH₂), 2.31 (t, 0.65H, oleic acid: α-CH₂), 2.17 (dt, 4H, oleoyl: α-CH₂), 2.10 (br q, 8H, oleoyl: CH₂-CH=CH), 1.88-1.55 (m, 2H, lysine, β-CH₂); (m, 2H, lysine, β-

CH₂); (m, 4H, lysine: δ-CH₂); (m, 4H, oleoyl: β-CH₂), 1.48 (t, 4H, diamine: 2,5-CH₂), 1.43 (s, 18H, Boc: CH₃), 1.41-1.20 (m, 4H, lysine: γ-CH₂); (m, 40H, oleoyl: CH₂); (m, 4H, diamine 3,4-CH₂), 0.88 (t, 6H, oleoyl: CH₃). LCQ (ESI) calculated (C₆₄H₁₂₀N₆O₈): 1100.9, found: 1101.5 (M+H)⁺, 1123.7 (M+Na)⁺. Optical rotation (10.27 mg in CHCl₃) [α] = -00.242, -00.233 g/mL.

2.2.3. Synthesis of (Oleoyl-Lys(H)-NH)₂(CH₂)₆·2HCl

Compound (**Oleoyl-Lys(Boc)-NH₂(CH₂)₆**) (115.3 mg, 0.105 mmol) was dissolved in 4 mL of CHCl₃ and added dropwise to 10 mL of 2 M HCl in ethyl acetate. The reaction mixture was stirred for 45 min and was regularly checked by TLC. After the reaction was finished, the solvent was evaporated partly under reduced pressure and a white precipitate appeared. Subsequently, *t*-butanol was added and the mixture was evaporated (two times) to remove the excess of HCl. The initial product (**Oleoyl-Lys(H)-NH₂(CH₂)₆·2HCl**) was obtained as a white solid in 98 % yield; this was subjected to one more column chromatography step to remove any residual oleic acid, yield: 238 mg (MW = 974.36, 93%) R_f = 0.19 (CHCl₃:MeOH = 5:1). ¹H NMR (300 MHz, DMSO-*d*₆) δ: 7.78-7.94 (m, 10H, NH), 5.35 (m, 4H, oleoyl CH=CH), 4.20 (q, 2H, lysine α-CH*), 3.05 (q, 4H, diamine 1,6-CH₂), 2.76 (q, 4H, lysine ε-CH₂), 2.15 (t, 4H, oleoyl α-CH₂), 2.01 (m, 8H, oleoyl CH₂-CH=CH), 1.45-1.70 (m, 4H, diamine 2,5-CH₂); (m, 4H, lysine δ-CH₂); (m, 4H, oleoyl β-CH₂); (m, 4H, lysine β-CH₂), 1.28-1.31 (m, 40H, oleoyl: CH₂); (m, 4H, diamine 3,4-CH₂); (m, 4H, lysine γ-CH₂), 0.89 (t, 6H, oleoyl CH₃). LCQ (ESI) calculated (C₅₁H₁₀₀N₆O₄): 900.8, found: 451.3 (M+2H)⁺, 901.6 (M+H)⁺.

2.3. Gene transfection experiments

2.3.1. Cell culturing

HeLa T-rex cells were grown in T75 bottles in EMEM+ (Eagles minimal essential medium containing 0.5% (vol.) PenStrep and 10% (vol.) Fetal Calf Serum (FCS) and 2 mM Glutamax-L) at 37 °C under a 5% CO₂ atmosphere and passed twice a week. Prior to transfection experiments, cells were washed, detached using trypsin and diluted 7.5-fold using EMEM+. Each well of a 6-well plate was then seeded with 2 mL of the cell suspension (~200.000 cells per well) and left to proliferate for one day before transfection experiments.

2.3.2. Preparation of the aggregates of the cationic lipids

For the positive control, 50 μL of DDAB and 50 μL of DOPE solutions in ethanol (6.6 mM and 13.2 mM, respectively) were mixed. Subsequently, this 100 μL ethanol solution was injected into 1.9 mL of milli-Q water and mixed by vortexing for 20 s at ambient temperature. The aggregates of the gemini surfactants used for transfection with the helper lipid DOPE were prepared in exactly the same way as the positive control, replacing DDAB with the gemini of interest. For studies without DOPE, the helper lipid was simply left out.

2.3.3. Preparation of the transfection complexes

As reporters for the transfection, plasmids (p-DNA) coding for either EGFP or β-galactosidase (β-gal) under a constitutive promoter were employed. For each well of a six-well plate 0.5 μg CMV β-gal plasmid and 0.5 μg EGFP plasmid were dissolved in

200 μl EMEM- (Eagles minimal essential medium containing 0.5% (vol.) PenStrep and 2 mM Glutamax-L but no Fetal Calf Serum). Transfection mixes as described above were then added as described in the legends of Figures 3, 4, 5, and 6, and the solution was allowed to incubate for half an hour.

2.3.4. Transfection using transfection complexes of cationic surfactants

The medium of the cells in the six-well plates was changed to 1 mL EMEM-. Subsequently, the transfection complexes were added and the mixtures were then left to incubate for 6 h at 37 °C under a 5% CO₂ atmosphere. After this period, the medium was removed and replaced by 2 mL EMEM+. The cells were then allowed to proliferate for two days.

2.3.5. Qualitative EGFP assay

To qualitatively assess transfection efficiency, a vector containing an EGFP gene under a constitutive promoter was transfected. This enabled simple fluorescence microscopy as a quick identifier of successful transfections, giving preliminary results based on fluorescence brightness.

2.3.6. Quantitative β -gal assay

Cells transfected with a constitutively expressed β -gal-coding gene had their medium removed and were subsequently lysed by incubation with 200 μl reporter lysis mix (RLM: 25 mM bicine, pH 7.5, 0.05% Tween-20 and 0.05% Tween-80 in water) for 15 minutes under continuous shaking. The lysates were then scraped and 20 μl was transferred to a perspex tube. Then 200 μl β -gal-mix (1% galacton, 5 mM MgSO₄, 100 mM phosphate buffer pH 8.0) was added to each tube, and the mixtures were left to incubate for 20 minutes. After this, 300 μl Accelerator II mix was added and the mixtures were incubated before the lysates were measured in a luminometer for 10 seconds per tube.

2.4. Physicochemical characterization

2.4.1. Electron Microscopy

Transmission electron microscopy (TEM) was carried out on dispersions prepared by sonication of the pure lipids (without DOPE) in water at 55 °C, which were allowed to dry on a carbon-formvar grid and stained with uranyl acetate. Because of the possible impact of the drying step in the sample preparation procedure for TEM, cryo-SEM (Scanning Electron Microscopy) was chosen for the investigation of the lipoplexes. Higher (approx. factor 40) lipid concentrations had to be used in order to be able to find good populations of aggregates in stead of one or some aggregates. A lipid solution of 6.70 mM in ethanol was prepared, of which 1 ml was evaporated in a rotary evaporator, resulting in a lipid film on the wall of the glass vessel. This was dispersed in 1 ml sterile milliQ water under vortexing for 20 s while heating till 50-60 °C.

2.4.2. Dynamic Light Scattering

Dynamic light scattering (DLS) is a much faster and less elaborate technique for screening the particle sizes than TEM or cryo-SEM, with no need for concentrated samples, so that the transfection solutions could be tested exactly as they were used in the transfection experiments. To remove dust and other large particles, however, the transfection solutions had to be filtered

prior to the DLS measurement; the pore size of the filtration Millipore frits was 200 nm. The measurements were performed on a Malvern Instruments Zetasizer Nano-S (ZEN 1600), equipped with a He-Ne laser (633 nm, 4 mW) and an Avalanche photodiode detector at an angle of 173°. The data were processed with Dispersion Technology Software (Malvern Instruments).

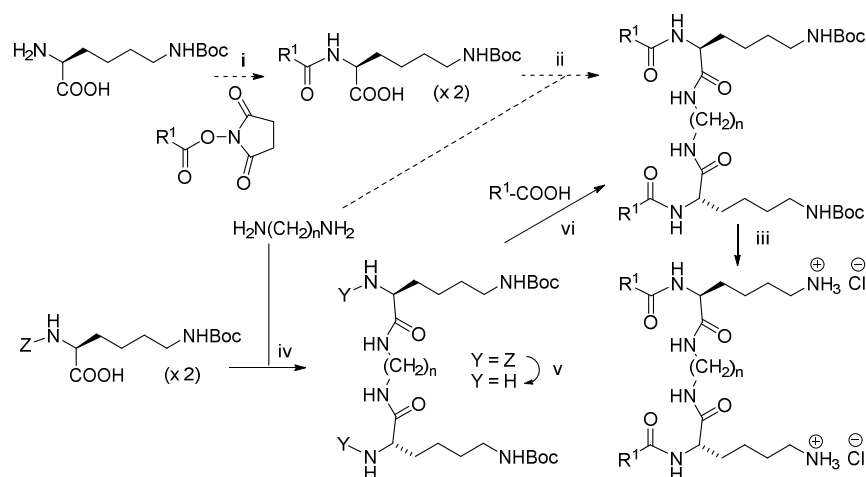
2.4.3. Small Angle X-ray Scattering

A surfactant was dispersed in milli-Q water, or phosphate buffer (pH 7), or phosphate/citrate buffer (pH 3) to a concentration in the 5 mM range. Lipoplexes were prepared by adding the appropriate amount of salmon sperm DNA solution to get N/P ratios between 1 and 7. SAXS experiments were conducted on the SAXS/WAXS station (BM26B) at the Dutch-Flemish beamlines (DUBBLE) at the European Synchrotron Radiation Facility in Grenoble, France [16,17]. During the experiments the ESRF was running at currents between 200 and 140 mA, and the monochromator was set at 1.24 Å (10 keV). The typical photon flux at the sample position with a beam size of 0.3 mm x 0.4 mm was 10⁹ photons/s. SAXS data of liposomes and lipoplexes in brass cells with mica windows were recorded with the gas multiwire 2-dimensional detector [18] at a sample to detector distance of 1.5 m. The background scattering due to solvent and empty cell was subtracted, and the spatial distortion and small inhomogeneities of the gas-filled detector (flat-field correction) were corrected for. Spatial calibration was performed with silver behenate [19] with an estimated error margin of $\pm 0.5\%$ in the observed periodicities.

3. Results and Discussion

3.1. Synthesis of the compounds (Oleoyl-Lys(H)-NH)₂(CH₂)_n

The synthesis of the class of compounds **Ol-Lys-H-n** with varying *n* is represented here by the compound with *n* = 6 as an example. The exploratory pathway for the preparation of **(R¹(CO)-Lys(H)-NH)₂(CH₂)_n** (dashed arrows in Scheme 1), which was used to prepare the compounds in our earlier report [5], involved acylation of the α -amino-group of lysine of which the ϵ -amino-group was Boc-protected, followed by activation of the lysine carboxylic acid group with ethyl chloroformate, coupling to the diamine, and subsequent deprotection of the Boc group. A similar approach was used in the synthesis of **C12-Lys-H-6** by others [10]. Although this 3-step procedure gave the HCl salts of the compounds **Ol-Lys-H-n** (*n* = 2, 4, 6, 8) in 10-25 % overall yield, it had a number of drawbacks with regard to the diastereomeric purity of the products. The first is that a technical grade of oleic acid was used, which contains 15-20 % of the *trans*-isomer (elaidic acid) besides the *cis*-isomer (oleic acid). In the preparation of gemini surfactants, the presence of such isomers can lead to a mixture of 3 stereoisomers, viz. the product with both tails *cis*, the product with both tails *trans*, and the product with 1 *cis* and 1 *trans* tail. Another problem is the use of the activated amino acid derivatives in combination with the basic conditions applied to prepare and couple them. Under basic circumstances the amino acids can racemize via the ketene intermediate, or, in the case of the *N*-acyl amino acid, via the cyclic oxazolone intermediate [20,21], in which the acidity of the hydrogen atom at the chiral center is enhanced. This leads to a mixture of products in which the two Lys residues either have



Scheme 1. General scheme for the preparation of $(R^1(\text{CO})\text{-Lys}(\text{H})\text{-NH})_2(\text{CH}_2)_n$. Dashed arrows refer to the published exploratory preparation [4], the solid arrows refer to the present work. i) 0.1 M NaOH in water/dioxane, 0 °C; b) $R^1(\text{CO})\text{-succinimide}$; ii) a) EtOCOC1, Et₃N, THF, -20 °C; b) $\text{H}_2\text{N}(\text{CH}_2)_n\text{NH}_2$; iii) 4 M HCl in EtOAc; iv) EDC•HCl, HOBT/EtOAc, H₂O; v) H₂, (Pd/C)/DMF; vi) $R^1\text{-COOH}$, EDC•HCl, HOBT/DMF.

both the natural L-configuration, or the D-configuration, or a product in which one lysine has the L-configuration and the other the D-configuration. This last product is a *meso* compound if the molecule is otherwise (i.e. with respect to the acyl substituent R^1) symmetrical.

In order to overcome these drawbacks a new synthetic route was designed in the present work (Scheme 1, solid arrows) in which the original problems were avoided. In this route, the order of reactions was changed. As the lysine was coupled first to the diamine via its carboxylic acid group (step iv), both its α - and ϵ -amines had to be protected with orthogonal groups, so Z-Lys(Boc)-OH was selected as the starting material. In the second step the Z group on the α -amine was selectively removed via hydrogenation (v) without affecting the Boc protection of the ϵ -amine [22]. After acylation of the unprotected α -amine (vi), the Boc protected ϵ -amine could be deprotected under acidic conditions (iii). The large increase in the optical rotation measured for **OI-Lys-H-6**, i.e. -14.0 ($c = 1.0$, MeOH) compared to -7.8 ($c = 0.92$, MeOH) for the product of the exploratory synthesis ([5], Scheme 1, top/dashed arrows) is a strong indication that epimerization had been largely prevented in the present case. A more detailed discussion of the synthetic approach is given in the Materials and Methods section and the Electronic Supplementary Information.

In the same way as described above for **OI-Lys-H-6**, the analogous compounds with spacer lengths 2, 3, 4, 5, 7, and 8 instead of 6 were also prepared, starting from protected enantiopure L-amino acids, and using the appropriate diamine in step iv. The analogues with varying acyl tails ($R^1(\text{CO})\text{-Lys}(\text{H})\text{-NH})_2(\text{CH}_2)_6$ (with $R^1 = \text{C18}$, stearoyl; C16, palmitoyl; C14, myristoyl; C12, lauroyl; C10, caprinoyl; C8, capryloyl; C18:1 (*E*), elaidoyl; and C18:2 (*Z, Z*), linoleoyl) were also prepared according to the procedure depicted in Scheme 1, using the appropriate carboxylic acid in step vi.

3.2. Transfection

3.2.1. Design of a protocol

The transfection abilities of the synthesized cationic gemini surfactants were investigated by studying the expression of

exogenous genes in cultured HeLa T-Rex cells in a protocol adapted from the literature [23]. The expression of the highly fluorescent enhanced green fluorescent protein (EGFP) [24] gave a quick qualitative indication of the transfection activity (Figure 2), that of beta-galactosidase (β -gal) [25], which could be analyzed with an assay for the enzymatic activity, gave a more accurate estimate of the transfection efficiencies. Such results are at best semi-quantitative, in view of the variation from experiment to experiment, and a positive control - DDAP/DOPE [26,27] in most experiments, Fugene [28] in our later experiments – was always included.

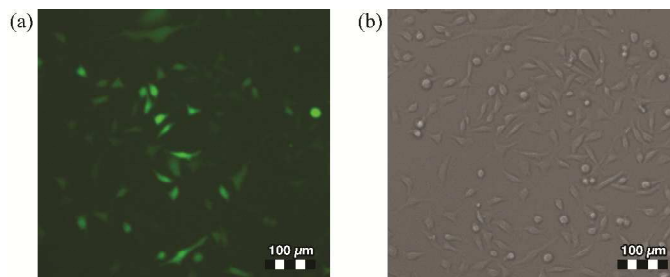


Figure 2. (a) Fluorescence and (b) corresponding light microscope image of the transfection of HeLa T-Rex cells by a vector coding for EGFP.

3.2.2. Optimization of the transfection parameters

The most active transfection agent in our exploratory study [5], the $n=6$ gemini surfactant **OI-Lys-H-6**, was used to optimize a number of variables for the transfection of HeLa T-rax cells with EGFP and β -gal vectors, viz. the ratio of positive charge in the lipid and negative charge in the nucleotide, the so-called ammonium/phosphate or N/P ratio, and the cationic lipid to ‘helper lipid’ or L/H ratio. The effect of the N/P ratio, which has a large influence on eventual toxicity of the transfection surfactant [29], was investigated with the same L/H ratio as that in the positive control, DDAB/DOPE, viz. 1/2. In Figure 3a there is a clear optimum corresponding to a N/P ratio of 1.27, implying that, assuming that all amines are protonated, there is a surplus of positive charge in the lipid-DNA complex (lipoplex). This would mean that after neutralizing all negatively charged phosphates

from the pDNA, some positive charge would remain to make the lipoplex positively charged and stick better to the negatively charged surface of the cell. This N/P ratio was subsequently used in the experiments in which the optimum L/H ratio was explored (Figure 3b), which was found to be at 1/2. The transfection efficiency using the L/H ratio of 1/1 in this experiment was very low, almost as low as the transfection efficiency that was obtained without any transfection solution.

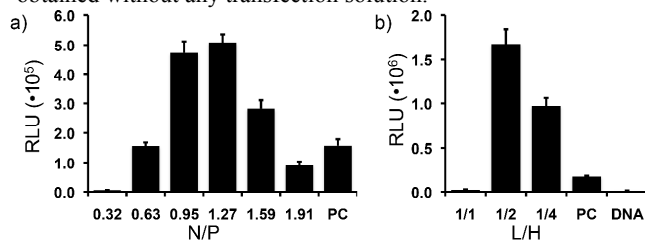


Figure 3. Transfection efficiencies in a β -gal assay with **Ol-Lys-H-6** and 1 μ g of pDNA (50% β -gal); PC, DDAB/DOPE positive control. (a) N/P ratio (amount of transfection solution per well) varied at L/H = 1/2. (b) L/H ratio varied at N/P = 1.27 with naked DNA without transfection mix (DNA) as a negative control.

In a separate experiment (not shown) we investigated whether the same transfection efficiencies could be achieved with less (viz. 0.5 or 0.25 mg) than 1 μ g pDNA per well for a six-well plate, but this turned out not to be the case. Improved transfection efficiencies could be obtained (not shown) if the transfection mix was not removed after 6 h, but instead retained in the HeLa cells by just adding the EMEM+ medium. We did not adapt our protocol in this direction, in order not to stimulate the transfection process beyond the count rate limitations of the β -gal assay. Only in the case when Fugene was used as a reference and positive control, this procedure of retaining the transfection mix was applied because the Fugene protocol [28] demanded so. All other experiments in the transfection series, i.e. those with DDAB/DOPE as a positive control, were performed using our standard protocol. We also found that transfection in a phosphate buffered solution tended to be somewhat higher than in sterile milli-Q water, but we found it more convenient to work with milli-Q because of the better stability of the transfection solutions in the refrigerator.

3.2.3. Transfection efficiencies for gemini surfactants with different spacer lengths

With the transfection protocol established and optimized for the **Ol-Lys-H-6**/DOPE transfection mixture, the series of different gemini surfactants could be tested for the influence of the spacer length on the transfection efficiencies. Figure 4a shows that there is little variation in the transfection efficiency as a function of the spacer length. Repeated experiments confirmed the subtle trend that the **Ol-Lys-H-n** compounds with $n = 2$ and in particular 3 are less active, while those with $n = 7$ and in particular 8 are more active than average. This result is an apparent contrast with that of the exploratory study [5], which indicated a pronounced transfection optimum for $n = 6$ compared to the compounds with $n = 4$ and $n = 8$. It should be noted, however, that those results were obtained on a different transfection system (luciferase in more easily transfectable CHO cells) without the helper lipid DOPE. We therefore investigated the transfection activity of the **Ol-Lys-H-n** surfactants without DOPE, with **Ol-Lys-H-6**/DOPE

as a positive control and reference. The results in Figure 4b show that, alone among this series, **Ol-Lys-H-6** showed a remarkable transfection activity without DOPE, in line with the exploratory results on CHO cells. Compared to the transfections with DOPE, the reproducibility of the transfections by **Ol-Lys-H-6** without DOPE was poor (not shown), possibly due to a lack of stability of the aggregates, but this was not further investigated.

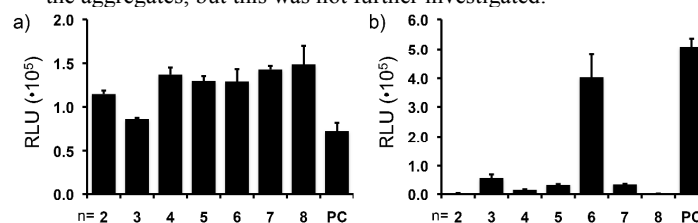


Figure 4. Transfection efficiency of the series **Ol-Lys-H-n** ($2 \leq n \leq 8$) with 1 μ g pDNA (50% β -gal) and 12 μ L of transfection solution (N/P = 1.27) per well. (a) with DOPE; PC, Fugene. (b) without DOPE; PC, **Ol-Lys-H-6**/DOPE=1/2.

3.2.4. The effect of the chirality on the transfection activity

Ol-Lys-H-6 was synthesized starting not only from natural L-lysine, but also from its enantiomer D-lysine. The resulting **Ol-D-Lys-H-6** appeared to be a somewhat better transfection agent (Figure 5a) than its L-enantiomer, in particular at an N/P ratio of 1.27. This difference in biological activity between the enantiomers must be due to a difference in diastereoisomeric interaction with the DNA, and with other chiral biomolecules such as membrane proteins and lipids. For another set of gemini surfactants, it has been shown that variations in the stereochemistry of chiral centres result in different interactions with DNA, and different transfection activities and toxicities [24]. Because we prefer the biodegradation products of our transfection agent to be as natural as possible we continued to work with L-lysine.

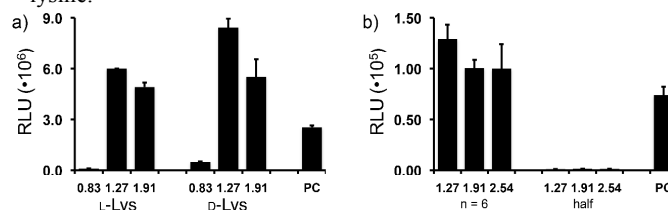


Figure 5. Transfection efficiencies for various amounts (N/P) of transfection mixtures using 1 μ g of pDNA (50% β -gal), L/H ratio 1/2, PC, Fugene. (a) Effect of chirality: **Ol-L-Lys-H-6** (left) vs. **Ol-D-Lys-H-6** (right) in PBS. (b) Effect of gemini structure: **Ol-Lys-H-6** (left) vs. half-gemini **Ol-Lys-NHEt** (right).

3.2.5. Gemini surfactant vs. half-gemini monomeric surfactant

Although most cationic lipids used in transfection studies discussed here so far have 2 alkyl tails [5], there are occasional examples where lipids with a single alkyl chain gave efficient transfections [31-33], with [34] or without DOPE [35]. One of these lipids resembles our gemini surfactant because it contains the amino acid ornithine (1 CH_2 group less than lysine) linked to oleyl alcohol by an ester bond [33]. It should be noted that the active single chain surfactants all have multiply charged headgroups. It is remarkable that there are only few cases where the efficiency of a cationic gemini surfactant has actually been compared to its monomeric counterpart [5, 36]. We therefore also

tested the monomeric surfactant analogue of **Ol-Lys-H-6** (lacking the spacer), the so-called half-gemini **Ol-Lys-NHEt**, for its transfection efficiency. As can be seen from Figure 5b, **Ol-Lys-H-6** (left) gave a nice transfection compared to the positive control at all amounts of transfection solutions, whereas the half-gemini **Ol-Lys-NHEt** (right, monomeric surfactant analogue) gave no transfection efficiency at all; omitting DOPE and increasing the amount of **Ol-Lys-NHEt** (not shown) did not improve this result. It can be concluded that the advantages of the gemini structure [5], as highlighted in the Introduction section, also apply to **Ol-Lys-H-6**, and are essential for transfection activity.

3.2.6. Effect of length and degree of unsaturation of the acyl tail

The effects of variation in the hydrophobic domain of cationic lipids on their physical properties have been thoroughly explored [31]. The structure of the hydrophobic domain determines the phase transition temperature and the stability of the formed liposomes at room temperature. Moreover, lipid membranes of high fluidity tend to promote fusion of bilayers, and hence increase the transfection efficiency [37,38]. Furthermore, the hydrophobic domain also contributes to the protection of the complexed DNA against nucleases and may contribute to the endosomal escape. Cationic surfactants with branched tails [39] or acetylenic tails [35,40] as well as with special sections like polyethylene glycol (PEG) [41,42] or fluorocarbon [43,44] regions in their hydrophobic chains have been reported in the literature. While the best hydrophobic tail for gemini surfactants is found to be the ole(o)yl tail, C18:1 (*Z*) [5], there are several reports on non-gemini surfactants that give higher transfection efficiencies with shorter saturated alkyl tails [45-48]. Moreover, **C12-Lys-H-6** has been shown to exhibit antimicrobial and haemolytic activities [10], and to form interesting condensed structures with DNA in a combined cryo-TEM and SAXS study [49]. These literature results prompted us to synthesize a series of gemini surfactants with saturated alkyl chains of different lengths and to test their transfection efficiencies using our general formulation and transfection protocol. As can be seen from Figure 6a, the transfection efficiencies for the gemini surfactants with the saturated tails were lower by 2 orders of magnitude at optimal concentrations, compared to **Ol-Lys-H-6** as a reference and positive control. Increasing the N/P ratio by adding more transfection mixture at equal amounts of pDNA per well did not improve the transfection efficiency, nor did varying the L/H ratio (data not shown). It has to be concluded that our (**R¹(CO)-Lys(H)-NH₂(CH₂)₆**) gemini surfactants with saturated acyl groups R¹(CO) are not active in transfection.

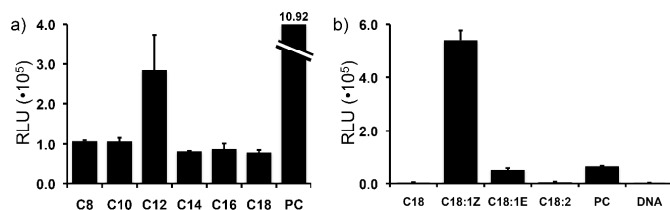


Figure 6. Transfection efficiency (β -gal assay) with L/H = 1/2, 12 μ L transfection solution per well (N/P = 1.27), and 1 μ g of pDNA. (a) Effect of length of acyl tail. PC, **Ol-Lys-H-6**/DOPE. (b) Effect of degree of unsaturation of acyl tail. PC, DDAB/DOPE.

Many biologically active gemini [5,36,50] and non-gemini surfactants [51] have one double bond in their hydrophobic C18 tails. It should be noted that, although often not explicitly mentioned, many synthetic procedures for the preparation of C18:1 containing surfactants start with a technical grade of oleic acid that contains 15-20 % elaidic acid. With few exceptions [52], the compound with the double bond in the *cis*-configuration (C18:1 *Z*, ole(o)yl) gave more efficient transfection when it was directly compared to the *trans* (elaidoyl) and the saturated (stearoyl) isomer [53,5]. For the so-called SAINT lipids [54,55], geminis [8], and geminoids [12], there are strong indications that the presence of *cis*-double bonds increases the fluidity of the lipids in the lipoplex, which in turn is an important factor in the efficiency of the DNA release from the lipoplexes upon encounter with (intra)cellular membranes. Because the phase transition temperature of the surfactants and the fluidity of the bilayer depend on the unsaturation in the alkyl tails, it was considered to be of interest to investigate what the effect of C18 tails with varying number and geometry of the double bonds would be in the series **R¹-Lys-H-6**. As can be seen in Figure 6b, the gemini surfactants containing oleoyl tails were by far superior to all other C18 tail containing gemini surfactants, when formulated with DOPE. For **C18-Lys-H-6** no real optimum for the transfection efficiencies could be detected (data not shown), mainly because the transfection efficiencies were too low. A transfection experiment using the elaidoyl containing gemini surfactants without the helper lipid DOPE did not show any significant transfection efficiency for various concentrations (data not shown). For the linoleoyl tail containing gemini surfactants no transfection efficiency was found at all, in spite of the fact that there are some reports [56,57] on transfection by cationic surfactants with more than one double bond in an alkyl tail. The most important result of this series of experiments is that it shows that for our gemini surfactant, oleoyl tails are superior to elaidoyl tails, in line with what was reported before for geminis in general [5], and with the aforementioned effect of the *cis* double bond on the membrane fluidity.

3.3. Physical properties of the surfactants

In order to gain more insight into the relation between transfection efficiency, as described in the previous section, on the one hand, and the molecular structure and aggregate formation on the other, the gemini surfactants were studied by a number of physical techniques, viz. by imaging (electron microscopy), scattering (dynamic light), and diffraction (with synchrotron X-rays).

3.3.1. Electron microscopy

Interesting morphological differences were observed with TEM within the **R¹-Lys-H-6** family of compounds (Figure 7). Flat structures, typical for bilayers [6], are found for the compounds with saturated tails (C18, here represented as stearoyl or St, Fig. 7a; C14, Fig. 7b) and mono-*E*-unsaturation (elaidoyl or El, Fig. 7c) where the bilayers have a tendency to roll up. Presumably, the alkyl tails of these compounds can easily adopt a linear conformation, which allows them to be packed tightly in a bilayer with little curvature. In contrast, the compound with mono-*Z*-unsaturated tails (oleoyl or Ol) formed vesicles (Fig. 7d), implying the formation of more strongly curved bilayers.

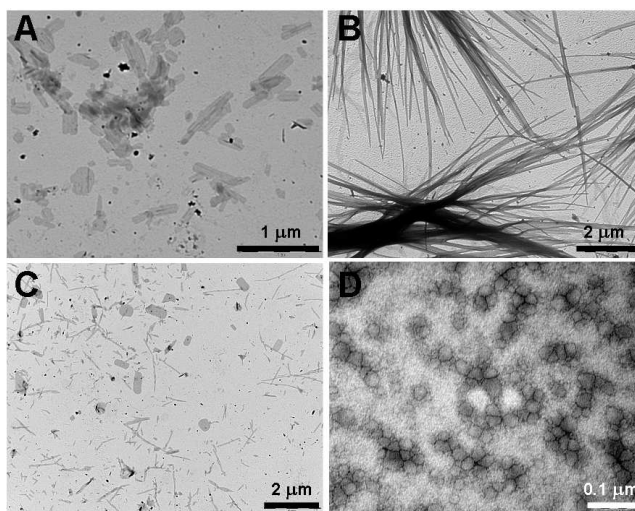


Figure 7. TEM pictures with negative staining by uranyl acetate (a) **St-Lys-H-6** (St = stearyl). (b) **C14-Lys-H-6**. (c) **E1-Lys-H-6** (E1 = elaidoyl). (d) **O1-Lys-H-6**.

For cryo-SEM, lipid dispersions of concentrations 40 times as high as those used in the transfection experiments were prepared. As can be seen from the micrographs of **O1-Lys-H-6** with DOPE in Figure 8, large amounts of aggregates were formed. Fig. 8B reveals that this particular sample was very polydisperse, with particle sizes ranging from small sized 60 nm-70 nm particles to very large vesicles of some 350 nm. In this picture it can be seen that some of the large aggregates have exploded in the vacuum of the cryo-SEM, thereby revealing the water containing lumen inside. This suggests that these large aggregates are big unilamellar vesicles, and not small multilamellar vesicles, in line with literature results [58].

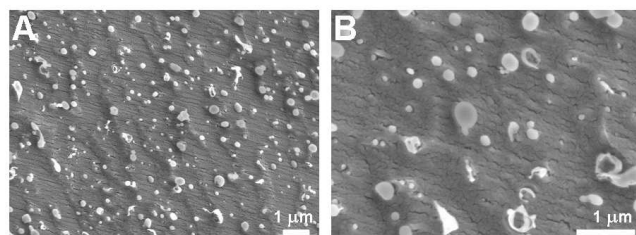


Figure 8. Cryo-SEM pictures of **O1-Lys-H-6**, L/H ratio $\frac{1}{2}$, at various magnifications.

3.3.2. Dynamic light scattering (DLS)

The results of the DLS experiments of the **O1-Lys-H-n** family are summarized in Table 1. The Z-average is the hydrodynamic radius (diameter in nm) of monodisperse spherical particles that correspond to the measured scattering; the PDI is the polydispersity index of the particles in the measured sample as calculated from the autocorrelation function, and the attenuator setting is a measure for the signal intensity (range: 1-11 in kcounts). The PDI values for the measurements on the mixtures with DOPE indicate that all samples are very polydisperse, but are still acceptable for a reliable measurement; the attenuator settings for these results are also acceptable.

Table 1. DLS results (diameter in nm, 25 °C) for the series **O1-Lys-H-n** (6.7 mM in milli-Q) with 2 molar equivalents of the helper lipid DOPE.

Spacer length (n)	With DOPE, L/H = 1/2		
	Z-average (nm)	PDI	Attenuator
2	56.36	364	9
3	74.95	257	8
4	58.75	264	9
5	89.77	231	7
6	76.78	231	8
7	83.06	248	8
8	114.3	228	7

The particle sizes measured for the mixtures of the surfactants with the helper lipid DOPE (ratio 1/2) correlate very roughly with the spacer lengths, increasing from 56 nm for **O1-Lys-H-2** to 114 nm for **O1-Lys-H-8**. Although it is not possible to relate the transfection efficiency (Fig. 4a) to the particle size of each surfactant, it is interesting to note that there is an underlying trend in which it increases with spacer length and particle size. Although the size measured by DLS is strictly a hydrodynamic radius, the results for $n = 6$ correlate very well with those of the cryo-SEM experiments (Figure 8), if we take into account that the larger aggregates in the DLS experiments are probably removed by the filtration step. The average particle size of the **O1-Lys-H-6** aggregates increased with increasing amounts of DOPE from 67 nm for a L/H ratio of 1/1 via 77 for L/H 1/2 (Table 1) to 91 and 97 nm for L/H 1/3 and L/H 1/4, respectively.

The DLS measurements on surfactants with different spacer lengths without DOPE, for which the transfection results were very poor, except for $n = 6$ (Figure 4b), suffered from a lack of signal, as reflected in the high values (11) for the attenuator setting; the PDI values (0.6-1.0) are also too high, which indicates that the values for the Z-average are based on a very poor fit. The problems may be explained in two ways. Either the particles are very small at the concentrations used, like in the case of small micelles, and not visible, or the particles are very large (> 200 nm) and were removed by the filtration step. In any case, the conclusion can be drawn that if no aggregates of a detectable size are formed, no or little transfection activity is measured, except for $n = 6$.

3.3.3. Small angle X-ray scattering (SAXS)

Small angle X-ray scattering (SAXS) experiments were carried out on dispersions of the free surfactants and on lipoplexes with N/P ratios of 3/1 and 1/1. In a number of cases, the pH and temperature dependences were also investigated. The results concerning the spacer and the tail dependence are given in Table 2 and shown in Figures 9 and 10.

Table 2. SAXS results for liposomes and lipoplexes of $R^I(\text{CO})\text{-Lys-H-n}$ ($d = 2\pi/q_{001}$, lamellar spacing; $a = 4\pi/\sqrt{3} \cdot q_{100}$, hexagonal or columnar spacing) at 25 °C. Ol, C18:1(Z) tails; El, C18:1(E) tails; St, saturated C18 tails.

R^I	n	pH	Free surfactant ^{a)}		Lipoplex N/P 3 ^{b)}			Lipoplex N/P 1		
			q (\AA^{-1})	d (\AA)	q (\AA^{-1})	d (\AA)	a (\AA)	q (\AA^{-1})	d (\AA)	a (\AA)
Ol	2	7	0.110, 0.236	57	0.106, 0.187, 0.215		68	106	59	
Ol	4	7	132	48	0.112, 0.196, 0.227		65	0.112, 0.197, 0.227		65
Ol	5	7	135	47	0.098, 0.112	64		111	57	
Ol	6	9	127	50	118	53		No peak		
Ol ^{c)}	6	7	126	50	118	53		111	57	
Ol ^{d)}	6	3	126	50	0.112, 0.138	56		0.112, 0.196, 0.227		65
Ol ^{e)}	1/2	7	106	59	105	60		104	60	
Ol	8	7	110	57	111	57		114	55	
El ^{f)}	6	7	139	45	115	55		105	60	
St	6	9	154	41	121	52		117	54	
St ^{g)}	6	7	169	39	117	54		105	60	
St ^{h)}	6	3	127	50	110	57		115	55	

a) Fig. 9a; b) Fig. 9b; c) Fig. 10a; d) Fig. 10b; e) $n = 1/2$, ‘half-gemini’ **Ol-Lys-NHET**; f) Fig. 10c; g) Fig. 10d; h) Fig. 10e.

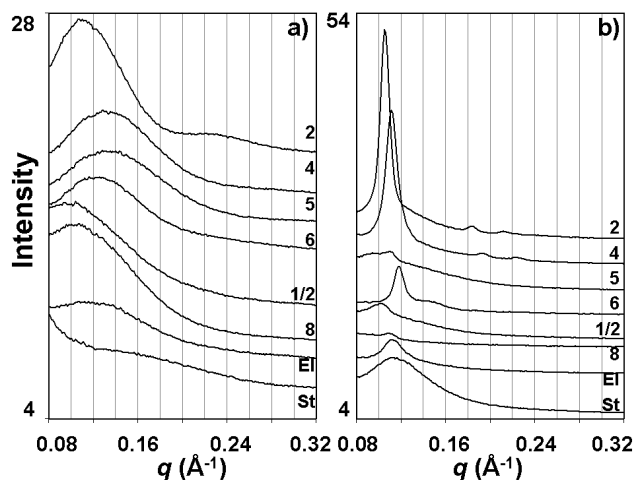


Figure 9. SAXS patterns for (a) liposomes and (b) lipoplexes (N/P 3) showing tail and spacer dependencies at 25 °C. Numbers 2, 4, etc. represent spacer length in **Ol-Lys-H-n**; 1/2 = ‘half-gemini’ **Ol-Lys-NHET**; El = Elaidoyl; St = Stearoyl.

For the new set of diastereomerically pure surfactants with $n = 6$, the position of the diffraction peak for elaidoyl surfactants at 45 Å is comparable to that found earlier [4] for a set of surfactants with natural oleic acid incorporated (45 Å), whereas that for (all-*cis*)-oleoyl surfactants is increased (50 Å, Table 2, left); in neither case were sharp diffraction patterns obtained (Figure 9a). The diffraction peaks are tentatively assigned to stacks of intercalated lipid bilayers (estimated molecular length 30 Å) of the liposomes of the free surfactants; the strong diffraction peak at low q is taken to represent the first order reflection, q_{001} , of a lamellar system with a periodicity d , or lamellar spacing, corresponding to

$= 2\pi/q_{001}$. For $n = 6$ at neutral pH, the bilayer thicknesses measured for the stearoyl and elaidoyl analogues (39 and 45 Å, respectively) are much lower than the bilayer thickness of the oleoyl surfactant (50 Å). This points to a much lower degree of surfactant intercalation in the bilayer structure in the latter case, which correlates nicely with the less tight packing of this surfactant as derived from the results of the electron microscopy study (Figure 7). For the oleoyl surfactants, the bilayer thicknesses for $n = 4$ and $n = 5$ (48 and 47 Å, respectively) are relatively small, which points to a large degree of intercalation of the surfactant tails comparable to that of the elaidoyl surfactant with $n = 6$ (45 Å). Relatively large bilayer thicknesses were found for the oleoyl surfactants with short ($n = 2$) and long ($n = 8$, both 57 Å) spacers. In most lipoplexes, the bilayer thickness increased compared to those of the liposomes, which indicates that the lipoplex consists of (alternating) lipid and DNA layers. For very short spacer lengths ($n = 2$, $n = 4$) a hexagonal phase was found at neutral pH; this is recognized by the occurrence of (110) and (200) reflections in addition to the (100) reflection, from which the hexagonal or columnar spacing a can be derived as $4\pi/\sqrt{3} \cdot q_{100}$. Also for $n = 6$ a hexagonal phase was found at pH 3 (Fig. 10b). These hexagonal phases could consist of cylindrical micelles of lipid with extended DNA molecules between them [59], or of an inverted structure with DNA at the center of a cylinder of lipid molecules [8].

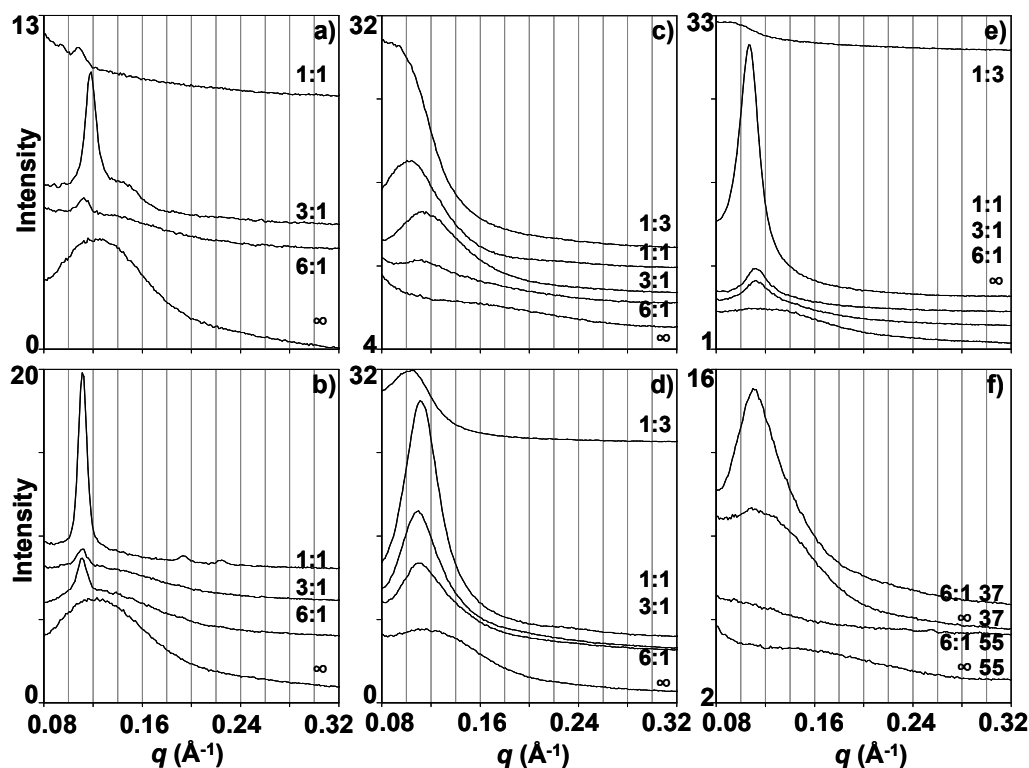


Figure 10. SAXS patterns for various N/P ratios including free surfactants (N/P ∞) at 25 °C (a-e). (a) and (b) **OI-Lys-H-6** at pH 7 and 3, respectively; (c) and (d) **C18-Lys-H-6** at pH 7 and 3, respectively; (e) **EI-Lys-H-6** at pH 7; (f) temperature dependence of **C18-Lys-H-6** at pH 3.

The amino groups of the lysine-based gemini surfactants have to be protonated in order to give positively charged groups that can have an electrostatic interaction with the negatively charged phosphate groups in DNA; because the pK_a values of two groups within a molecule are different and both are shifted to lower pH when the lipid molecules aggregate, the interaction with DNA can be expected to be pH dependent in a pH range that is relevant for the effectivity of the transfection, in particular when this occurs by a mechanism of DNA condensation followed by endocytosis. It has been reported earlier that the pH dependence of the complex of DNA and cationic lipids can result in transitions between lamellar and hexagonal packings of the resulting lipoplex which can trigger the endosomal escape [8], and the tendency for a surfactant to form the hexagonal phase has been taken as an explanation for the efficiency of some gemini-like surfactants to give good transfection without helper lipids [9,60]. In the present series of results, the aforementioned findings of hexagonal phases for the lipoplexes of some of the **OI-Lys-H-n** gemini surfactants do not appear to correlate well with the transfection activities in the absence of helper lipid; they are found for $n = 2$, $n = 4$, and $n = 6$, of which only $n = 6$ is active without helper lipid (Figure 5a). The results do make sense in the context of the proposed model for endosomal escape when the pH is considered: the hexagonal phase found for $n = 6$ at pH 3 may be a good explanation for the efficiency of this surfactant without helper lipid (Figure 5b), whereas the hexagonal phase found for $n = 2$ and 4 at neutral pH apparently is not an advantage for an efficient transfection.

It is of interest to note (Table 2) that pH changes do not affect the **OI-Lys-H-6** liposomes (Figure 10a-b) but that the

bilayer thickness of **St-Lys-H-6** liposomes increases from 39 to 50 Å upon lowering the pH from neutral to 3 (Figure 10c-d). Surprisingly, the increased charge on the gemini headgroup due to the protonation of both amines results in a decreased intercalation of the surfactant tails. The bilayer initially becomes even thicker when the temperature is increased to 37 °C (from 50 to 57 Å) but at higher temperatures decreases to values characteristic of strong intercalation (37 Å at 55 °C, Fig. 10f; 39 Å at 70 °C). The structures of the corresponding liposomes were hardly affected by the temperature variation. The temperature dependence of a number of lipoplexes with sharp diffraction peaks was also investigated. The columnar spacing of the **OI-Lys-H-2** lipoplex (N/P 3) varies subtly but significantly with temperature, starting at 68.1 Å at 25 °C to a maximum value of 69.1 Å at 37 °C and then back to 67.1 Å at 55 °C and 66.6 Å at 70 °C; a similar observation was made for the **OI-Lys-H-4** lipoplex (N/P 3; a values are 64.7, 65.3, 64.8, and 62.5 Å, respectively).

4. Conclusions

The exploratory synthesis of lysine-based gemini surfactants of the type $(R^1(CO)-Lys(H)-NH)_2(CH_2)_n$, on which we reported earlier [4], led to products that may have contained up to 10 stereoisomers, including two meso compounds and two pairs of enantiomers, due to the use of technical oleic acid, combined with a racemization-prone synthetic protocol. A new strategy was therefore followed in the present study, starting from pure oleic acid. Lysine-based gemini surfactants of the type $(R^1(CO)-Lys(H)-NH)_2(CH_2)_n$ with $R^1 =$ oleoyl and $n = 2-8$ were successfully synthesized. Transfection studies showed

that the gemini surfactant with $n = 6$ was the biologically most active compound. Therefore, the corresponding enantiomeric compound starting from D-lysine was also prepared, as well as L-lysine derived analogues with $n = 6$ containing hydrophobic tails varying in length ($R'(CO) = C8, C10, C12, C14, C16, \text{ and } C18$) and degree of unsaturation ($C18:1 E$ and $Z, C18:2 (Z,Z)$). The 'half gemini' (monomeric surfactant analogue) was prepared by incorporating aminoethane.

The potential of the gemini surfactants to transfer polynucleotides across cell membranes was investigated by transfection of HeLa cells with beta-galactosidase with and without the presence of the helper lipid DOPE. Oleoyl ($C18:1(Z)$) was by far the best hydrophobic tail for obtaining high biological activity, whereas the effect of the lysine stereochemistry was less pronounced. Only in the absence of helper lipid an optimum spacer length ($n = 6$) was observed. The gemini structure was essential; the 'half-gemini' (monomeric surfactant analogue) was less active by 2 orders of magnitude. The most active surfactant **Oleoyl-Lys(H)-NH₂(CH₂)₆**, formed liposomes with sizes in the range 60 – 350 nm. Its lipoplex with N/P ratio 1 underwent a transition from a lamellar to hexagonal morphology upon lowering the pH from 7 to 3 in the absence of helper lipid, a morphological change which is consistent with endosomal escape triggered by lowering of the pH.

Acknowledgements

The authors thank the ENGEMS network for supporting the initial phase of this work, and the Dutch Research Council (NWO) for facilitating the SAXS investigations at the DUBBLE beam line. The Nijmegen Molecular Biology department (Siebe van Genesen, Prof. N. H. Lubsen) are acknowledged for transfection facilities and valuable discussions. The research was funded by the Dutch Technology Foundation STW (M.D., grant stw.06565). R.J.M.N acknowledges support from the Ministry of Education, Culture and Science (Gravity program 024.001.035).

Notes and references

^a *Radboud University Nijmegen, Institute for Molecules and Materials, Heijendaalseweg 135, 6525 AJ Nijmegen, The Netherlands. Fax: +31-24-3652929; Tel.: +31-24-3652016; E-Mail: m.feiters@science.ru.nl*

^b *DUBBLE CRG/ESRF, Netherlands Organization for Scientific Research (NWO), c/o ESRF BP 220, F38043 Grenoble Cedex, France*

[#] *Present address: Diamond Light Source Ltd, Didcot OX11 0DE, Oxon, England, UK*

† Electronic Supplementary Information (ESI) available: [details of any supplementary information available should be included here]. See DOI: 10.1039/b000000x/

Abbreviations:

BAW, butanol : acetic acid : water = 4 : 1 : 1 (v/v/v); β -gal, β -galactosidase; Boc, *t*-butyloxycarbonyl; CMC, critical micelle concentration; CMV, cytomegalovirus; DCHA, dicyclohexylammonium; DDAB, didodecyl ammonium bromide; DMF, *N,N*-dimethylformamide; DLS, dynamic light scattering; DNA, desoxyribonucleic acid; DOPE, dioleoylphosphatidyl ethanolamine; EDC, Ethylene dimethylamino-propyl carbodiimide; EGFP, enhanced green fluorescent protein; El, elaidoyl; EM, electron microscopy; EMEM, Eagle's minimum essential medium; EMEM+, EMEM with FCS; FCS, fetal calf serum; FID, Free Induction Decay; HOBt, 1-hydroxybenzotriazole; LCQ-ESI, (liquid chromatography) quadrupole

electrospray ionisation mass spectrometry; L/H, molar lipid/helper lipid (DOPE) ratio; L/P, molar lipid/phosphate ratio; mRNA, messenger RNA; NMR, nuclear magnetic resonance; N/P, molar positively charged nitrogen/negatively charged phosphate ratio; Ol, oleoyl; PC, positive control; PBS, phosphate buffered saline; pDNA, plasmid DNA; RLM, reporter lysis mix; RLU, relative luminescence units; SAXS, small angle X-ray scattering; SEM, scanning electron microscopy; St, stearoyl; TFA, trifluoroacetic acid; TLC, thin layer chromatography; Z, carboxybenzyl.

‡ Footnotes should appear here. These might include comments relevant to but not central to the matter under discussion, limited experimental and spectral data, and crystallographic data.

- 1 F. M. Menger, C. A. Littau, *J. Am. Chem. Soc.* **1991**, *113*, 1451-1452.
- 2 R. Zana, *J. Coll. Interf. Sci.* **2002**, *248*, 203-220.
- 3 A. Bajaj, P. Kondaiah, S. Bhattacharya, *J. Med. Chem.* **2008**, *51*, 2533-2540.
- 4 M. J. Rosen, *ChemTech* **1993**, *23*, 30-33.
- 5 A. J. Kirby, P. Camilleri, J. B. F. N. Engberts, M. C. Feiters, R. J. M. Nolte, O. Söderman, M. Bergsma, P. C. Bell, M. L. Fielden, C. L. García Rodríguez, P. Guédát, A. Kremer, C. McGregor, C. Perrin, G. Ronsin, M. C. P. van Eijk, *Angew. Chem. Int. Ed.* **2003**, *42*, 1448-1457.
- 6 P. J. J. A. Buynsters, C. L. García Rodríguez, E. L. Willighagen, N. A. J. M. Sommerdijk, A. Kremer, P. Camilleri, M. C. Feiters, R. J. M. Nolte, B. Zwanenburg, *Eur. J. Org. Chem.* **2002**, 1397-1406.
- 7 M. Mammen, S.-K. Choi, G. M. Whitesides, *Angew. Chem. Int. Ed.* **1998**, *37*, 2754-2794.
- 8 P. C. Bell, M. Bergsma, I. P. Dolbnya, W. Bras, M. C. A. Stuart, A. E. Rowan, M. C. Feiters, J. B. F. N. Engberts, *J. Am. Chem. Soc.* **2003**, *125*, 1551-1558.
- 9 L. Pérez, J. L. Torres, A. Manresa, C. Solans, M. R. Infante, *Langmuir* **1996**, *12*, 5296-5301.
- 10 A. Colomer, A. Pinazo, M. A. Manresa, M. P. Vinardell, M. Mitjans, M. R. Infante, L. Pérez, *J. Med. Chem.* **2011**, *54*, 989-1002.
- 11 A. Colomer, A. Pinazo, M. T. Garcia, M. Mitjans, M. P. Vinardell, M. R. Infante, V. Martínez, L. Peréz, *Langmuir* **2012**, *28*, 5900-5912.
- 12 M. Damen, J. Aarbiou, S. F. M. van Dongen, R. M. Buijs-Offerman, P. P. Spijkers, M. van den Heuvel, K. Kvashnina, R. J. M. Nolte, B. J. Scholte, M. C. Feiters, *J. Control. Release* **2010**, *145*, 33-39.
- 13 I. Koltover, T. Salditt, J. O. Rädler, C. R. Safinya, *Science* **1998**, *281*, 78-81.
- 14 G. Caracciolo, D. Pozzi, H. Amenitsch, R. Caminiti, *Langmuir*, **2005**, *21*, 11582-11587.
- 15 M. Muñoz-Úbeda, A. Rodríguez-Pulido, A. Nogales, A. Martín-Molina, E. Aicart, E. Junquera, *Biomacromolecules*, **2010**, *11*, 3332-3340.
- 16 W. Bras, An SAXS/WAXS beamline at the ESRF and future experiments, *J. Macromol. Sci.-Phys. B* **1998**, *37*, 557-565.
- 17 M. Borsboom, W. Bras, I. Cerjak, D. Detollenaere, D.G. van Loon, P. Goedtkindt, M. Konijnenburg, P. Lassing, Y.K. Levine, B. Munneke, M. Oversluizen, R. van Tol, E. Vlieg, *J. Synchrotron Rad.* **1998**, *5*, 518-520.
- 18 A. Gabriel, F. Dauvergne, *Nucl. Instr. Meth.* **1982**, *201*, 223-230.
- 19 T.C. Huang, H. Toraya, T.N. Blanton, Y. Wu, *J. Appl. Cryst.* **1993**, *26*, 180-184.
- 20 S. Doonan, *Peptides and proteins*, Royal Society of Chemistry (Great Britain), Edward W. Abel, Royal Society of Chemistry, **2002**, p. 37 (ISBN 0854046925, 9780854046928)
- 21 J. H. Jones, M. J. Witty, *J. Chem. Soc. Chem. Commun.* **1977**, *125*, 281-282.
- 22 M. Bergmann, L. Zervas, *Ber. Deutschen chem. Ges.* **1932**, *65*, 1192-1201.
- 23 L. Doerwald, S. T. van Genesen, C. Onnekink, L. Marin-Vinader, F. de Lange, W. W. de Jong, N. H. Lubsen, *Cell. Mol. Life Sci.* **2006**, *63*, 735-743.

- 24 G. H. Zhang, V. Gurtu, S. R. Kain, *Biochem. Biophys. Res. Commun.* **1996**, *227*, 707-711.
- 25 J. Alam, J. L. Cook, *Anal. Biochem.* **1990**, *188*, 245-254.
- 26 M. J. Campbell, *Biotechniques* **1995**, *18*, 1027-1032.
- 27 C. R. Dass, T. Walker, M. A. Burton, *Drug Deliv.* **2002**, *9*, 11-18.
- 28 <http://labs.mmg.pitt.edu/gioerup/Fugene6.pdf>
- 29 M. Muñoz-Ubeda, S. K. Misra, A. L. Barrán-Berdón, C. Aicart-Ramos, M. B. Sierra, J. Biswas, P. Kondaiah, E. Junquera, S. Bhattacharya, E. Aicart, *J. Am. Chem. Soc.* **2011**, *133*, 18014-18017.
- 30 S. Aleandri, M. G. Bonicelli, F. Bordi, S. Casciardi, M. Diociaiuti, L. Giansanti, F. Leonelli, G. Mancini, G. Perrone, S. Sennato, *Soft Matter* **2012**, *8*, 5904-5915.
- 31 D.-F. Zhi, S.-B. Zhang, B. Wang, Y.-N. Zhao, B.-L. Yang, S.-J. Yu, *Bioconjugate Chem.* **2010**, *21*, 563-577.
- 32 P. Pinnaduwaage, L. Schmitt, L. Huang, *Biochim. Biophys. Acta* **1989**, *985*, 33-37.
- 33 F. H. Cameron, M. J. Moghaddam, V. J. Bender, R. G. Whittaker, M. Mott, T. Lockett, *Biochim. Biophys. Acta* **1999**, *1417*, 37-50.
- 34 F. Tang, J. A. Hughes, *J. Controlled Release* **1999**, *62*, 345-358.
- 35 M. Patel, E. Vivien, E. Hauchecorne, N. Oudrhiri, R. Ramasawmy, J.-P. Vigneron, P. Lehn, J.-M. Lehn, *Biochem. Biophys. Res. Commun.* **2001**, *281*, 536-543.
- 36 C. McGregor, C. Perrin, M. Monck, P. Camilleri, A. J. Kirby, *J. Am. Chem. Soc.* **2001**, *123*, 6215-6220.
- 37 J. O. Rädler, I. Koltover, T. Salditt, C. R. Safinya, *Science* **1997**, *275*, 810-814.
- 38 R. Zantl, L. Baicu, F. Artzner, I. Sprenger, G. Rapp, J. O. Rädler, *J. Phys. Chem. B* **1999**, *103*, 10300-10310.
- 39 M. E. Ferrari, D. Rusalov, J. Enas, C. J. Wheeler, *Nucleic Acids Res.* **2002**, *30*, 1808-1816.
- 40 S. Fletcher, A. Ahmad, E. Perouzel, A. Heron, A. D. Miller, M. R. Jorgensen, *J. Med. Chem.* **2006**, *49*, 349-357.
- 41 S. Bhattacharya, P. V. Dileep, *Tetrahedron Lett.* **1999**, *40*, 8167-8170.
- 42 S. Bhattacharya, P. V. Dileep, *Bioconjugate Chem.* **2004**, *15*, 508-519.
- 43 J. Gaucheron, C. Santaella, P. Vierling, *Bioconj. Chem.* **2001**, *12*, 114-128.
- 44 K. Fabio, C. Di Giorgio, P. Vierling, *Biochim. Biophys. Acta* **2005**, *1724*, 203-214.
- 45 R. P. Balasubramaniam, M. J. Bennett, A. M. Aberle, J. G. Malone, M. H. Nantz, R. W. Malone, *Gene Therapy* **1996**, *3*, 163-172.
- 46 V. Floch, M. P. Audrezet, C. Guillaume, E. Gobin, J. G. Le Bolch, J. C. Clement, J. J. Yaouanc, H. Des Abbayes, B. Mercier, J. Leroy, J. F. Abgrall, C. Ferec, *Biochim. Biophys. Acta* **1998**, *1371*, 53-70.
- 47 H. S. Kim, J. Moon, K. S. Kim, M. M. Choi, J. E. Lee, Y. Heo, D. H. Cho, D. O. Jang, y. S. Park, *Bioconj. Chem.* **2004**, *15*, 1095-1101.
- 48 J. A. Heyes, D. Niculescu-Duvaz, R. G. Cooper, C. J. Springer, *J. Med. Chem.* **2002**, *45*, 99-114.
- 49 A. L. Barrán-Berdón, M. Muñoz-Ubeda, C. Aicart-Ramos, L. Pérez, M.-R. Infante, P. Castro-Hartmann, A. Martín-Molina, E. Aicarta, E. Junquera, *Soft Matter* **2012**, *8*, 7368-7380.
- 50 M. L. Fielden, C. Perrin, A. Kremer, M. Bergsma, M. C. Stuart, P. Camilleri, J. B. F. N. Engberts, *Eur. J. Biochem.* **2001**, *268*, 1269-1279.
- 51 D. Liu, T. Ren, X. Gao, *Curr. Med. Chem.* **2003**, *10*, 1005-1013.
- 52 I. van der Woude, A. Wagenaar, A. A. P. Meekel, M. B. A. ter Beest, M. H. J. Ruiters, J. B. F. N. Engberts, D. Hoekstra, *Proc. Natl. Acad. Sci. U. S. A.* **1997**, *94*, 1160-1165.
- 53 S. Obika, W. Yu, A. Shimoyama, T. Uneda, K. Miyashita, T. Doi, T. Imanishi, *Bioorg. Med. Chem.* **2001**, *9*, 245-254.
- 54 J. Šmisterová, A. Wagenaar, M. C. A. Stuart, E. Polushkin, G. Ten Brinke, R. Hulst, J. B. F. N. Engberts, D. Hoekstra, *J. Biol. Chem.* **2001**, *276*, 47615-47622.
- 55 I. S. Zuhorn, V. Oberle, W. H. Visser, J. B. F. N. Engberts, U. Bakowsky, E. Polushkin, D. Hoekstra, *Biophys. J.* **2002**, *83*, 2096-2108.
- 56 J. Heyes, L. Palmer, K. Bremner, I. MacLachlan, *J. Control. Release* **2005**, *107*, 276-287.
- 57 B. Yu, S.-H. Hsu, C. Zhou, X. Wang, M. C. Terp, Y. Wu, L. Teng, Y. Mao, F. Wang, W. Xue, S. T. Jacob, K. Ghoshal, R. J. Lee, L. J. Lee, *Biomater.* **2012**, *33*, 5924-5934.
- 58 M. Muñoz-Ubeda, A. Rodríguez-Pulido, A. Nogales, O. Llorca, M. Quesada-Pérez, A. Martín-Molina, E. Aicart, E. Junquera, *Soft Matter* **2011**, *7*, 5991-6004.
- 59 L. Wasungu, M. C.A. Stuart, M. Scarzello, J. B. F. N. Engberts, D. Hoekstra, *Biochim. Biophys. Acta* **2006**, *1758*, 1677-1684.
- 60 R. Koynova, B. Tenchov, *Soft Matter* **2009**, *5*, 3187-3200.

Table of contents text:

Lysine-based gemini surfactants with mono-unsaturated tails transfected without helper lipid because of the ability of the lipoplex to change morphology with pH

Table of contents graph

